Three Dimensional Bearing Capacity of Shallow Foundations Adjacent to Slopes Using Discrete Element Method

Mona Arabshahi monaarabshahi@gmail.com
Graduate Student of Soil Mechanics and Foundation Engineering
School of Civil Eng., College of Engineering, University of Tehran

Ali Asghar Mirghasemi aghasemi@ut.ac.ir
Associate Professor
School of Civil Eng., College of Engineering
University of Tehran

Ali Reza Majidi armajidi@gmail.com
Ph.D. of Soil Mechanics and Foundation Engineering
Mahab Ghodss Consulting Engineers

ABSTRACT

In the current study, an effort is made to determine three dimensional bearing capacity of a shallow foundation adjacent to a slope using discrete element method. The soil mass under the footing is modeled as discrete blocks connected with a set of normal and shear springs called Winkler springs. In order to define the geometry of the failure surface of the soil, six independent angles are considered, which will be obtained by trial and error. So, the failure surface is not fixed and can be changed by different characters.

The purpose of the paper is to determine the three dimensional bearing capacity coefficients of rectangular foundations which are placed adjacent to a slope. In order to get to such a scope a discrete element program called BCAP3D (Bearing capacity analysis program in 3D) is employed. The result is presented in relative graphs, versus the ratio ($\frac{x}{B}$), for each foundation aspect ratio ($\frac{L}{B}$). Besides, a comparison is made between the current method with other methods used in the same field.

Keywords: 3 Dimensional, Bearing Capacity, Shallow Foundations/Footings, Discrete Element Method.

1. INTRODUCTION

1-1 Field of The Research

Bearing capacity of foundations has always been one of the most interesting research subjects in geotechnical engineering. In such a field of study, extensive efforts have been made for bearing capacity in two dimensions. It seems that 2D theoretical approaches have reached to a relatively satisfactory level for ordinary loading and soil conditions. Considering that real foundations are not infinitely long and their failure mechanism is certainly three dimensional, it is necessary to study the real conditions and try to develop analytical 3D estimations of the bearing capacity.

Among the researches in 3D bearing capacity, a few of them consider the effect of the ground inclination or a nearby slope in reducing the ultimate load of the footing, which is the main subject of the current paper.

1-2 Previous Studies

Evaluation of the 3D bearing capacity of shallow foundations is usually assessed by introducing experimental and empirical shape factors into the ordinary 2D equations for the strip footings developed by researchers such as Meyerhof [1], Terzaghi and Peck [2], Hansen [3], de Beer [4], Vesic [5], and the others.

The general bearing capacity relationship suggested by these researches can be expressed as:

$$q_{ult} = cN_c + qN_q + 0.5\gamma BN_\gamma \quad (1)$$

Where N_c, N_q and N_γ are the bearing capacity coefficients in two dimensional state. For considering the effect of the lateral surfaces in three dimensional conditions, the experimental related shape factors will be used.

In order to employ analytical methods in such a research, Shield and Drucker [6] presented a theoretical evaluation of 3D bearing capacity of rectangular foundations on homogeneous clay ($\varphi = 0$) by means of upper and lower bound solutions. Nakase [7] used a limit equilibrium method and assumed cylindrical sliding surfaces for rectangular footings on normally consolidated clays. Narita and Yamaguchi [8], presented a three dimensional analysis of bearing capacity of rectangular foundations by means of the method of slices, assuming that sliding surfaces are composed of a set of log-spirals with different initial radii. There are plenty of other researches in different conditions such as works of Ugai [9], Michalowski [10], Michalowski and Dawson [11], Zhu and Michalowski [12] and Salgado et al. [13].

Askari and farzaneh [14] used an upper bound method to determine the bearing capacity of strip foundations near slopes. Sarma and Chen [15] also studied the same problem during earthquake using a limit equilibrium technique.

1-3 History of The Discrete Element Method

Cundall and Strack [16] established a Discrete Element Method to study the micromechanical behaviour of granular materials by modelling assemblies of two dimensional circular particles. In this method each particle is considered as a distinct (discrete) element.

The new concept of DEM presented here, falls within the framework of the limit equilibrium methodology. In two dimensional state, this method was presented by Chang for analysis of bearing capacity of foundations [17], slope stability [18] and retaining walls [19]. Using this method, soil mass is modelled as a system of blocks connected together by elasto-plastic Winkler springs. So in the current method, every block is considered as a discrete element.

The former state of DEM is an explicit method and the latter one is an implicit method.

1-4 Using DEM for 3D bearing capacity

Majidi and Mirghasemi [20] employed the DEM to study the 3D bearing capacity of rectangular foundations. The same method is used here to obtain the 3D bearing capacity of footings adjacent to slopes.

2. DISCRETE ELEMENT MODEL

The method used in order to achieve the 3D bearing capacity coefficients of a foundation is briefly introduced in here.

2-1 General Information and main equations

To determine the three dimensional bearing capacity of rectangular shallow foundations by DEM, it is assumed that the soil mass beneath the footing consists of several discrete blocks connected with an infinite number of Winkler springs, as shown in Fig. 1. As the load applied on the footing increases, these blocks are going to slip in order to define the failure mechanism.

Each group of Winkler springs consists of three sets of springs in different orthogonal directions (Fig.2). One set of springs is located in the direction normal to the contact surface to simulate the normal stiffness of the soil (E) and the two other sets are placed within the contact surface, perpendicular to each other, to behave as shear stiffness (G) of the soil.

The behaviour of the normal and shear springs is assumed to be Elasto-Plastic. As shown in Fig. 3, the normal springs do not yield in compression. However, in tension they would yield at the tensile capacity.

Also, based on Mohr-Coulomb failure criteria, the shear springs yield when the shear strength (τ_p) is reached, as:

$$\tau_p = c + \sigma_n \tan\varphi \quad (2)$$

The initial values of stiffness in the normal and shear directions between blocks can be estimated using Young's modulus (E) and shear modulus (G), respectively [18]. According to the soil behaviour, no tension will appear in normal spring and just shear springs will result in failure of the soil when they reach their shear resistance. Whenever the force in a shear spring reaches its ultimate value, the initial shear stiffness (k_{shear}) will be substituted by the reduced secant shear stiffness (k'_{shear}). (Fig. 3-b)

The present method can be used to model progressive failure of a sliding soil mass. As the applied load increases, the induced stresses in springs may exceed the allowable stresses. When the shear stress is beyond the admissible stress at an interface, the local factor of safety is set to be 1 for the interface and the iteration process redistributes the excessive amount of stress to the neighbouring blocks. The iterative procedure is carried out until the stresses at all interfaces of blocks are compatible with their deformations and completely satisfy the stress-displacement relationships.

In discrete element method, the constraint information is given on the centers of blocks. So, it is necessary to determine the relative displacement of two adjacent blocks according to the center of their interface. Due to the relative displacement between two neighbouring blocks, the springs are deformed and their stresses can be calculated. By integrating on each surface of the blocks, the relative force will be obtained. The forces acting on all sides of a block should satisfy the force and displacement equilibrium requirement. The relationship between the forces and the displacements for all blocks can be written as:

$$\{f\} = [K]\{U\} \quad (3)$$

Where [K] is the global stiffness of the system and the vectors {*f*} and {U} consist of body forces and displacements for all blocks, respectively.

Solving the equation (3), normal and shear forces between blocks will be obtained and so, the overall safety factor of the system can be defined through equation (4).

$$S.F = \frac{\sum \tau_{pi} A_i}{\sum \sqrt{(\tau_{si})^2 + (\tau_{ti})^2}.A_i} \quad (4)$$

Where τ_{pi} is the shear strength of the soil and τ_{si} and τ_{ti} are the existing shear stresses on the failure surface.

2-2 The Geometry of The Failure Surface

The failure mass of the soil below the footing consists of three zones similar to the classical 2D bearing capacity failure surface (Mirghasemi and Majidi, [21]). Each of them can be divided into several wedges as shown in Fig. 4.

The failure mechanism contains of an active zone below the footing (zone I), which is pushed downward into the soil mass and a passive wedge (zone III) moves laterally. The transition between downward movement of the active zone and lateral movement of the passive zone takes place through the radial shear zone (II). The shape of the failure surface of zone (II) is assumed to be a logarithmic spiral. The shape of the failure surface is a function of the footing width (B) and length (L), the internal friction angle of the underlying soil (φ) and the six independent angles of α_1, α_2, α_3, α_4, θ_1 and θ_2.

The angles θ_1 and θ_2 as shown in the Fig. 4-b, determine the inclination of lateral failure surfaces in the three dimensional space. The absolute values of θ_1 and θ_2 are assumed to be identical ($|\theta_1 = \theta_2|$) due to the symmetry in the foundation geometry and loading.

These six angles are not predefined and will be obtained by iteration in order to get the most critical failure surface. So, a large number of failure surfaces would be examined to determine the ultimate bearing capacity of the footing.

2-3 General Assumptions

In order to determine the ultimate bearing capacity of a shallow foundation adjacent to a slope by DEM, it is necessary to clarify the assumptions used in the analyses. They can be mentioned as:

1. The blocks are rigid and just relative displacement of adjacent blocks will be taken into account.
2. Every two adjacent blocks will remain in contact and no separation would be occurred.
3. The load is applied to a rectangular rigid foundation with the dimensions $B \times L$.
4. Loading is vertical and centric.
5. The general shear failure will occur in the soil mass.
6. The dry soil density is used.
7. There is a distance (x) between the footing and the edge of the slope which its inclination angle is β.
8. In order to obtain the 3D bearing capacity coefficients, the superposition method has been taken into account.
9. The surcharge applying to the ground is defined just on one side of the foundation where the failure mechanism would be constructed. No surcharge will be considered on the inclined ground surface.
10. The radial shear zone (II) is assumed to be divided into 10 blocks. Also, it's better for zones (I) and (III) to model as a single block due to their non-shear behaviour [20].

Fig.5 shows the position of a failure mechanism in the relation to the slope inclination.

3. COMPARISON TO OTHER METHODS

3-1 Compare to Classical methods

To compare the 3D bearing capacity of shallow foundation near the slopes resulted from DEM with other methods, the results of two classic semi-empirical methods which presented by Hansen [3] and Vesic [5] are used. Fig. 6 to Fig. 8 shows the bearing capacity of a footing on top of a slope of inclination (β) where: $\frac{x}{B} = 0$.

3-2 Compare to AASHTO LRFD Bridge Design Specification

AASHTO LRFD bridge design specifications suggests some empirical factors and graphs to determine the bearing capacity of foundations near slopes, for cohesionless soils and for saturated clays, separately. [22]
A comparison between the ultimate bearing capacities resulted from DEM and LRFD specifications is made and shown in Fig. 9 to Fig. 12.

3-3 Compare to experimental results

A comparison is made between the bearing capacity resulted from DEM and an experimental research of a square footing near a slope [23]. A footing of $10\text{cm} \times 10\text{cm}$ is places near a slope of 25° inclination. The soil properties are:

$\varphi = 32°, c = 0.2\ {}^{ton}/_{m^2}$

Table 1 shows the comparison between these two methods.

4. THREE DIMENSIONAL BEARING CAPACITY COEFFICIENTS

A nearby slope will definitely decrease the bearing capacity of a rectangular foundation. In the current study, the bearing capacity coefficients are achieved using DEM with mentioned assumptions. The results are presented for each of the coefficients versus the dimensionless quantity ($\frac{x}{B}$), for different foundation aspect ratios.

The bearing capacity can be obtained through the equation:

$$q_{ult} = cN_{cm} + qN_{qm} + 0.5\gamma BN_{\gamma m} \quad (5)$$

In which N_{cm}, N_{qm} and $N_{\gamma m}$ are the modified 3D bearing capacity coefficients of the rectangular foundation near a slope.

4-1 The coefficient of soil cohesion (N_{cm})

In order to have N_{cm}, we can obtain the bearing capacity of a weightless soil and disregarding the surcharge on the ground. Figs. 13 to 24 indicate the factor of N_{cm}.

4-2 The coefficient of soil weight ($N_{\gamma m}$)

$N_{\gamma m}$ can be defined as the bearing capacity of a cohesionless soil of density equals to $2\ ton/m^3$ and disregarding the surcharge on the ground. Figs. 25 to 36 indicate the factor of $N_{\gamma m}$. These Figures are provided for the situation: $\beta \leq \varphi$.

4-3 The coefficient of surcharge (N_{qm})

To obtain N_{qm}, the weight and cohesion of the soil should be disregarded. Figs. 37 to 40 indicate the factor of N_{qm}, for all the slope inclination.
The analyses indicate that N_{qm} is hardly a function of the slope inclination and for various slope inclinations N_{qm} varies in a small range. This is because of the definition of the surcharge in the current method.
As the surcharge on the ground is defined to the edge of the slope, for a certain ($\frac{x}{B}$) the amount of surcharge would be constant for every quantity of slope inclination. So, the only difference is a small decrease in the failure length of the third region in the failure mechanism, as the angle of the slope inclination increases.

4-4 Influence of The Foundation Aspect Ratio

An analysis is made to study the effect of the foundation aspect ratio on the bearing capacity of the footing. As it is shown in Fig. 41 and 42, increasing in footing aspect ratio ($\frac{L}{B}$) results in the decrease of the bearing capacity. This is because of the fact that as the foundation aspect ratio increases, the influence of the lateral failure surfaces on the bearing capacity decreases. And finally, it reaches its 2D ultimate value.

5. SUMMARY AND CONCLUSIONS

In this research, analyses based on Discrete Element Method (DEM) are carried out for determining three dimensional bearing capacity coefficients of shallow foundations near slopes. By determining the parameters through relative sensitivity analyses, the final analyses are made to get 3D bearing capacity coefficients. Besides, a comparison to other methods that can determine the 3D bearing capacity of a shallow foundation near a slope is made.
The results obtained from the present study can be summarized as follows:

1. The results of the present method are to some extent in accordance with classical semi-empirical results proposed by earlier researchers such as Hansen and Vesic. The present DEM will results in less bearing capacities compare to the classical methods.
2. DEM will results in higher value of bearing capacities comparing to AASHTO LRFD specifications. However, the difference isn't a great deal.
3. For higher values of foundation aspect ratios, the comparison between different methods results in less differences for bearing capacities.

4. Just like other methods, the bearing capacity coefficients obtained by DEM are highly dependent on the internal friction of the soil, especially for φ values greater than 30°.

5. For each value of the slope inclination, there is a critical x value which for $x \geq x_{critical}$ the slope has no effect on the failure mechanism and bearing capacity of the foundation. This critical distance can be found in the graphs provided for bearing capacity coefficients.
6. The critical x described above, will decrease by decreasing in the soil friction angle. It also will increase by increasing in foundation aspect ratio.
7. As can be seen in the graphs, for slope inclination more than 30°, N_c will decrease more slowly in comparison to inclinations less than 30°.

6. Tables and Figures

Difference (%)	Q (DEM) $(^{ton}/_{m^2})$	Q (experimental) $(^{ton}/_{m^2})$	x/B	Soil density $(^{ton}/_{m^2})$
13.8	9.05	10.5	0.3	1.61
11.2	7.1	8.0	0.3	1.51

Table. 1: Comparison between DEM and experimental bearing capacity

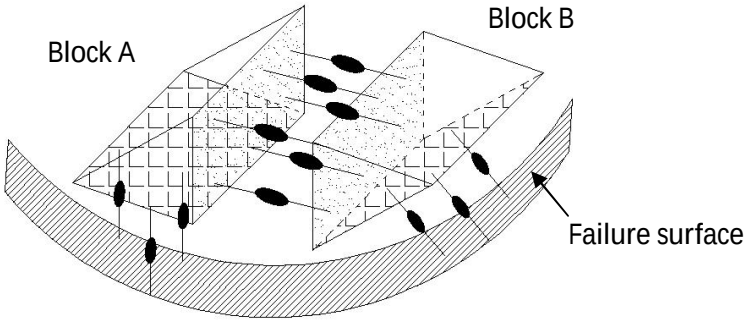

Fig.1: Connection of the blocks with the Winkler springs

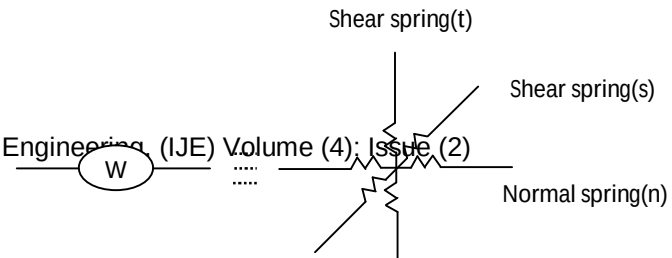

Fig.2: A Winkler spring is consists of three perpendicular springs

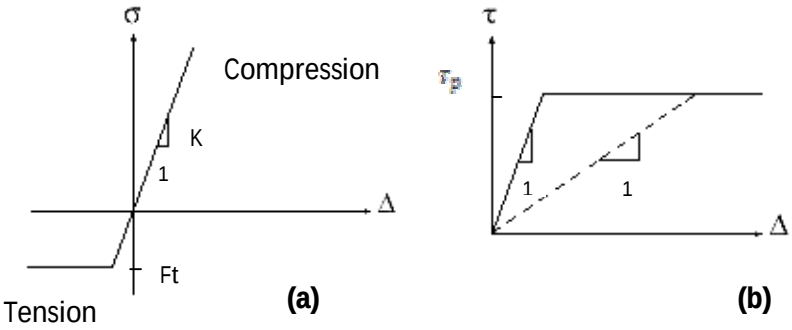

Fig.3: The behaviour of normal (a) and shear (b) springs

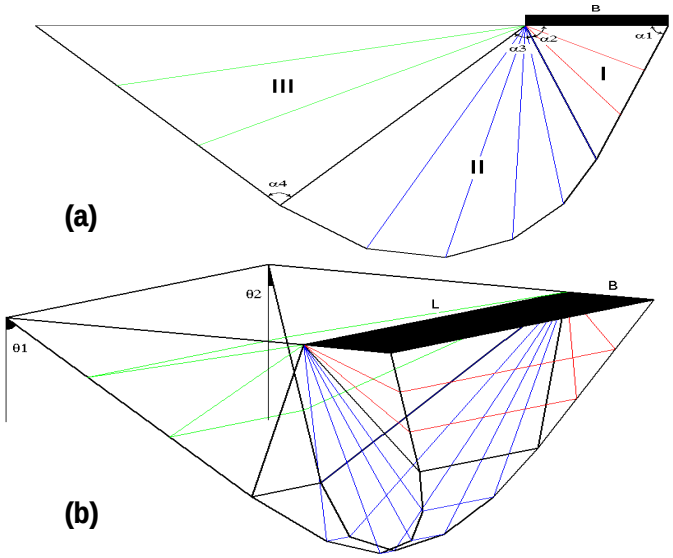

Fig.4: The failure surface below the footing (a) 2D view (b) 3D view

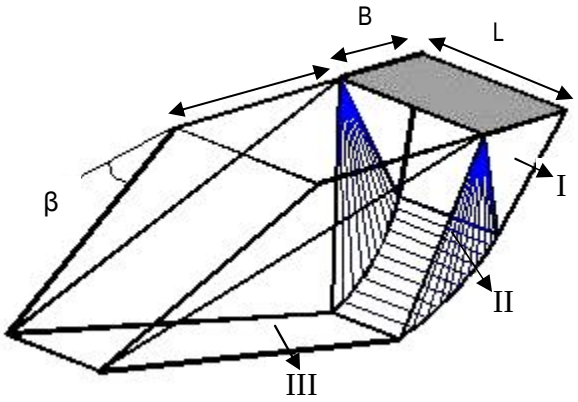

Fig.5: The position of the footing and the slope

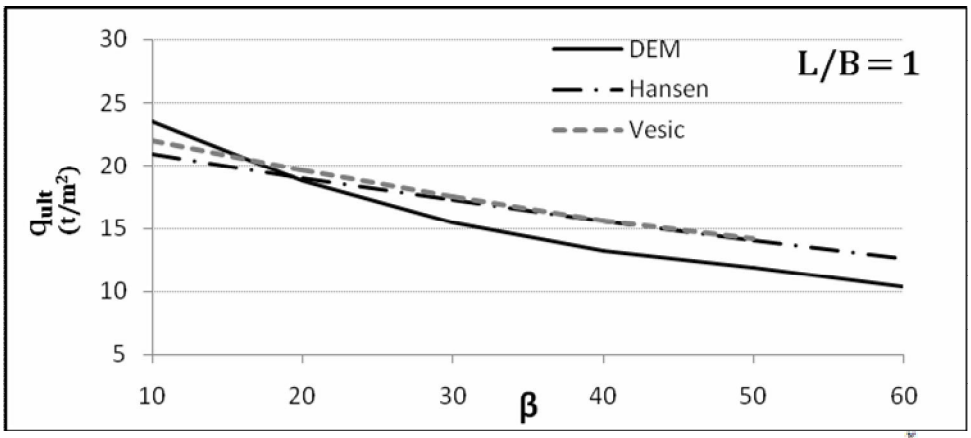

Fig. 6: Comparison of the bearing capacity resulted from DEM and Classic methods ($\frac{\kappa}{B} = 0, \varphi = 20$)

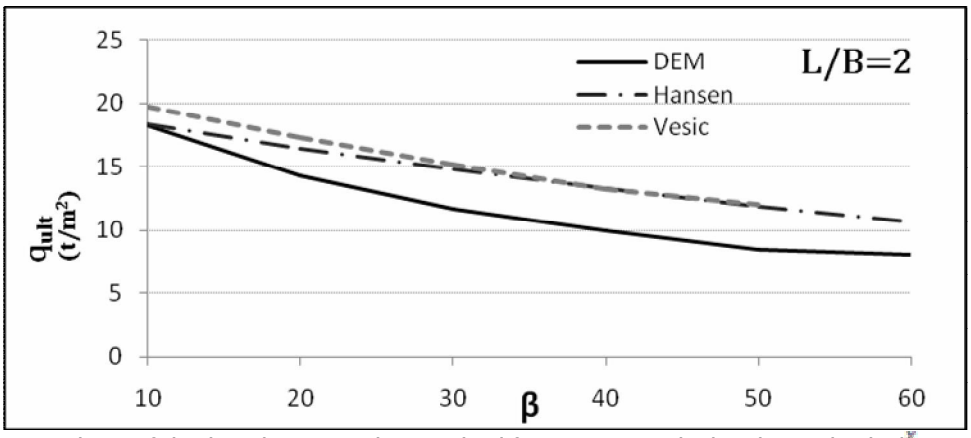

Fig. 7: Comparison of the bearing capacity resulted from DEM and Classic methods ($\frac{\kappa}{B} = 0, \varphi = 20$)

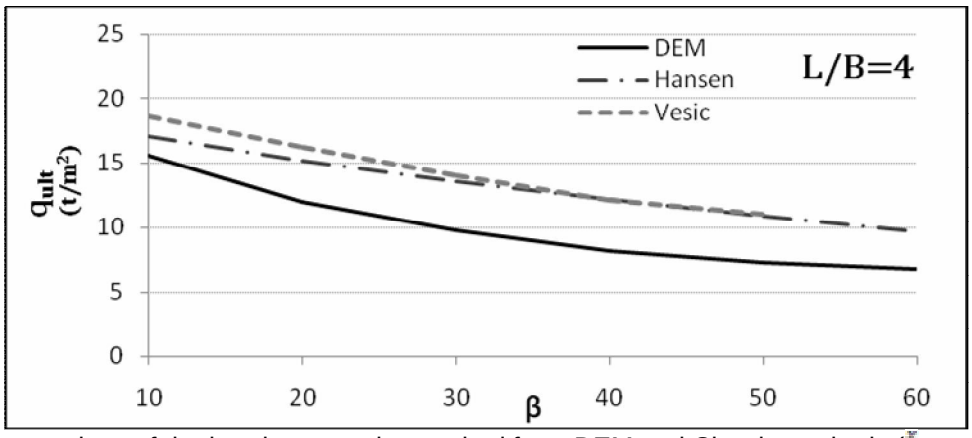

Fig. 8: Comparison of the bearing capacity resulted from DEM and Classic methods ($\frac{x}{B} = 0, \varphi = 20$)

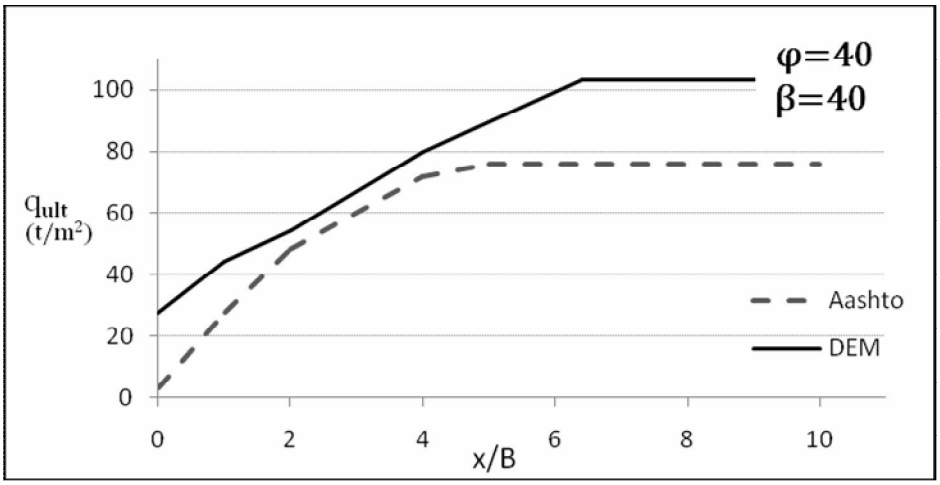

Fig. 9: Comparison of the bearing capacity of cohesionless soil resulted from DEM and AASHTO ($\frac{L}{B} = 2$)

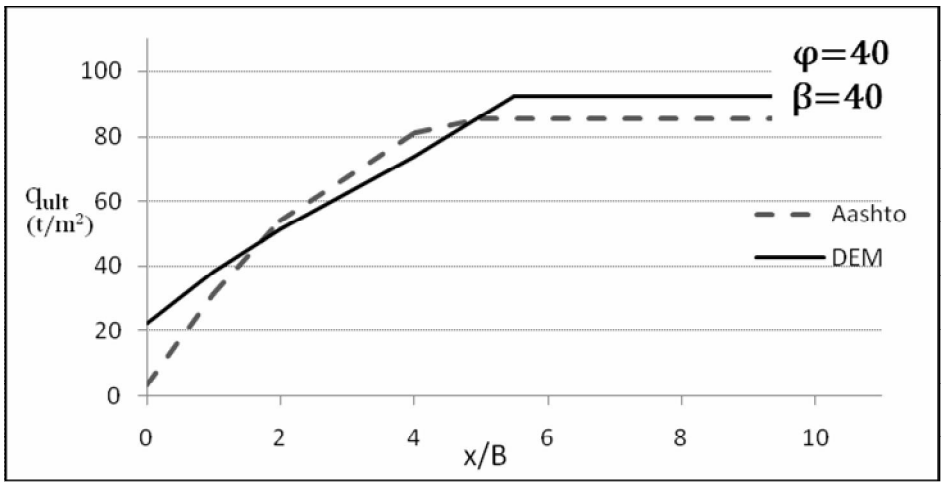

Fig. 10: Comparison of the bearing capacity of cohesionless soil resulted from DEM and AASHTO ($\frac{L}{B} = 4$)

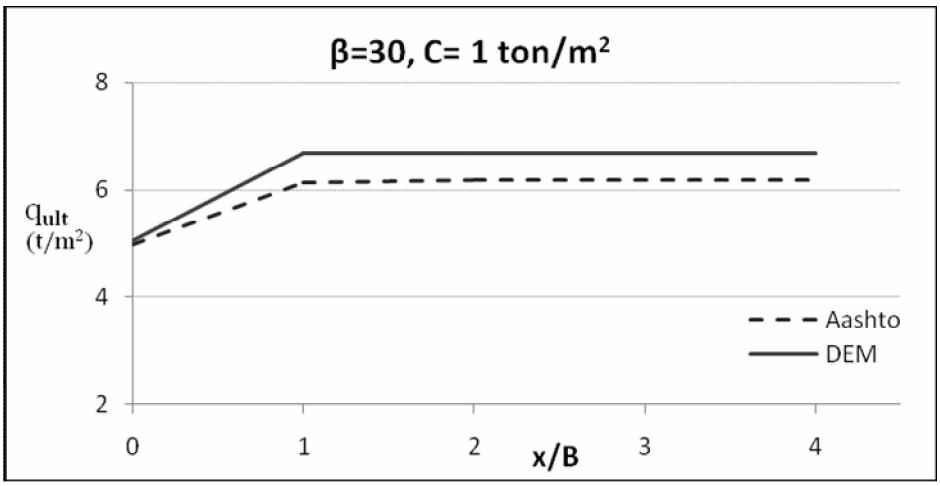

Fig. 11: Comparison of the bearing capacity of saturated clay resulted from DEM and AASHTO ($\frac{L}{B} = 1$)

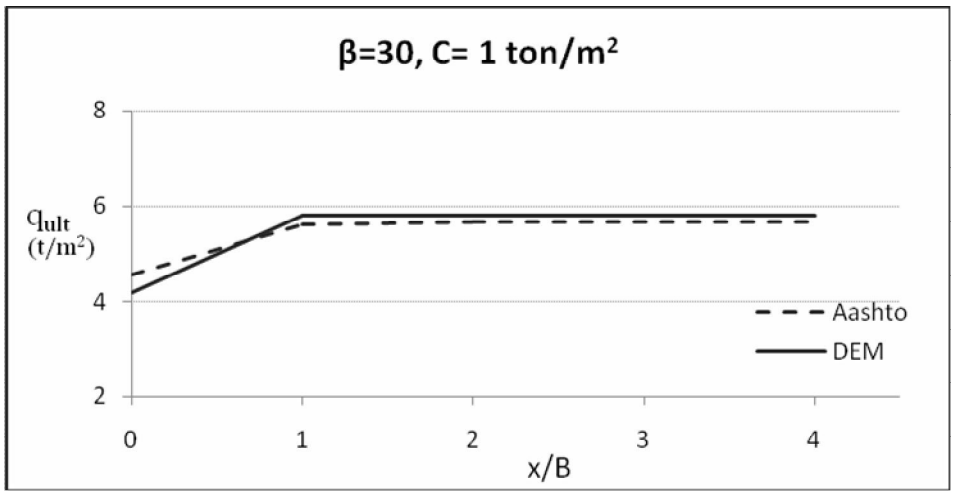

Fig. 12: Comparison of the bearing capacity of saturated clay resulted from DEM and AASHTO ($\frac{L}{B} = 2$)

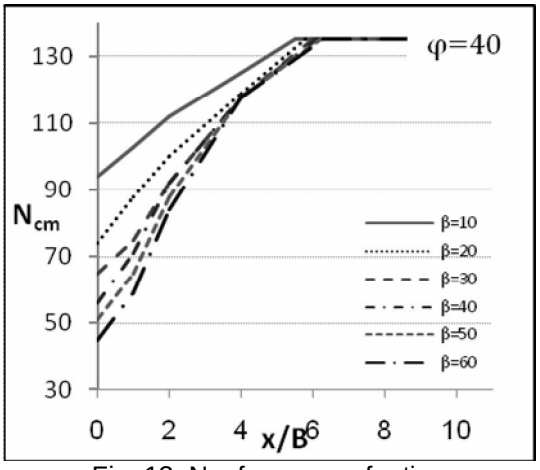

Fig. 13: N_{cm} for square footing

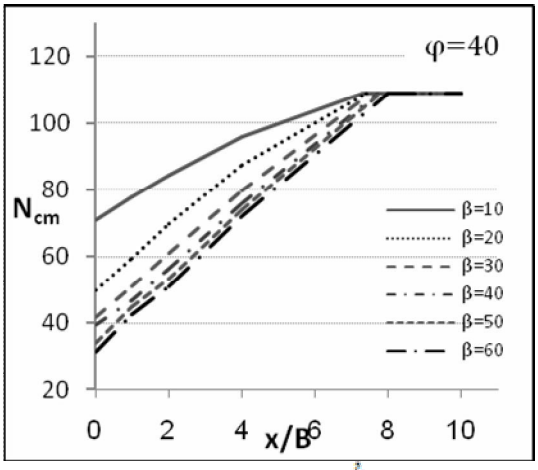

Fig. 16: N_{cm} for ($\frac{L}{B} = 2$)

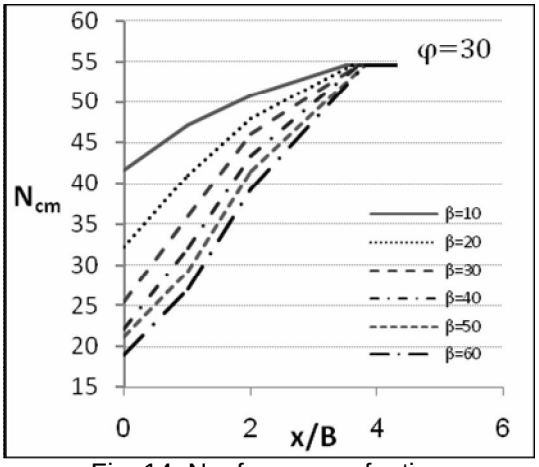

Fig. 14: N_{cm} for square footing

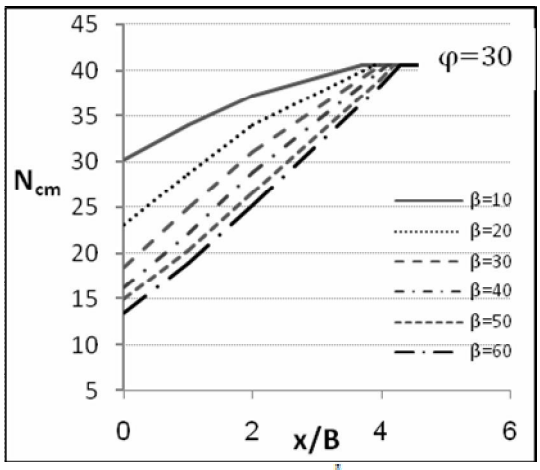

Fig. 17: N_{cm} for ($\frac{L}{B} = 2$)

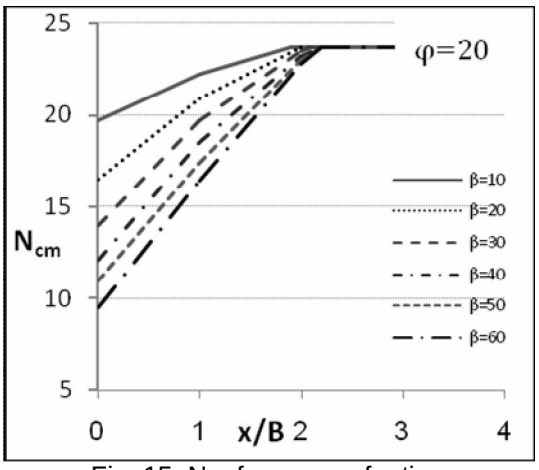

Fig. 15: N_{cm} for square footing

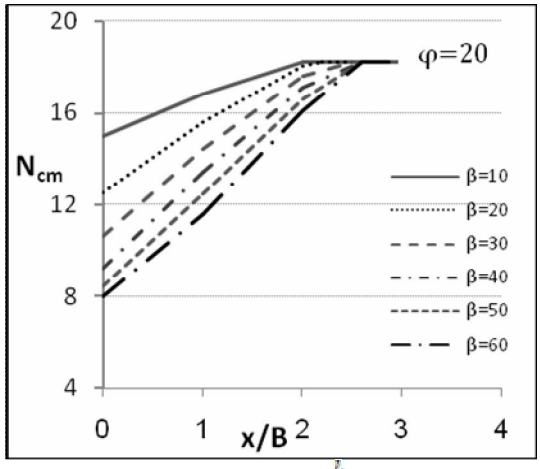

Fig. 18: N_{cm} for ($\frac{L}{B} = 2$)

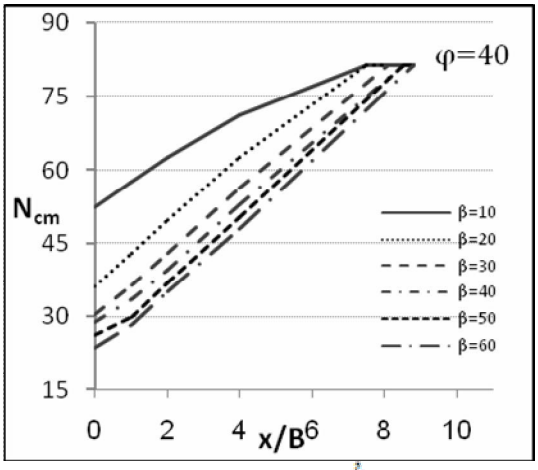

Fig. 19: N_{cm} for ($\frac{L}{B} = 4$)

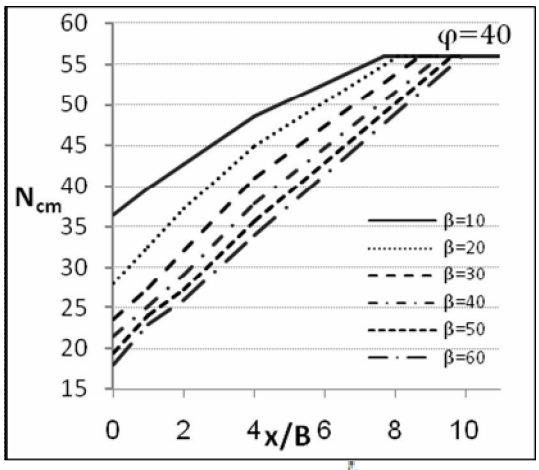

Fig. 22: N_{cm} for ($\frac{L}{B} = 10$)

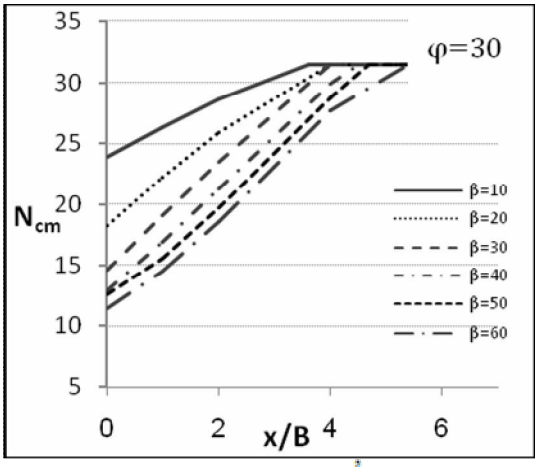

Fig. 20: N_{cm} for ($\frac{L}{B} = 4$)

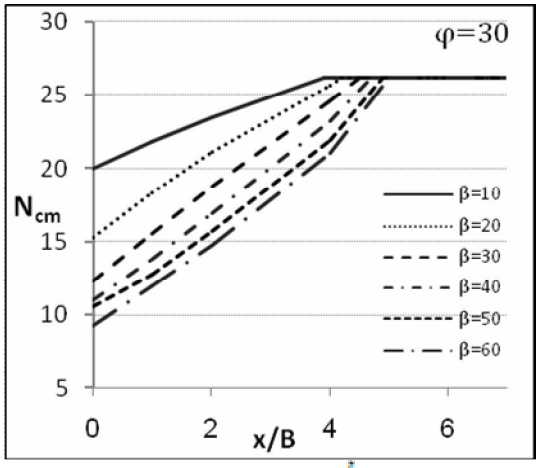

Fig. 23: N_{cm} for ($\frac{L}{B} = 10$)

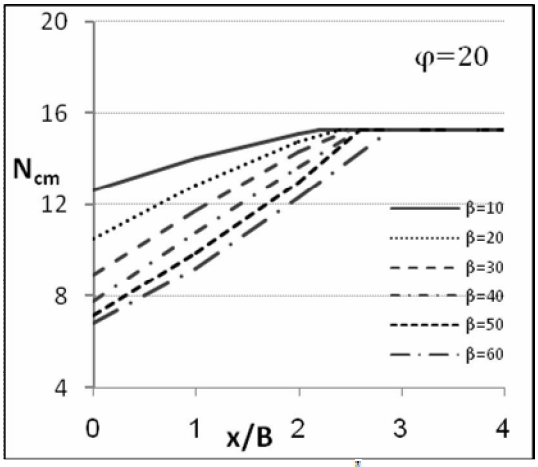

Fig. 21: N_{cm} for ($\frac{L}{B} = 4$)

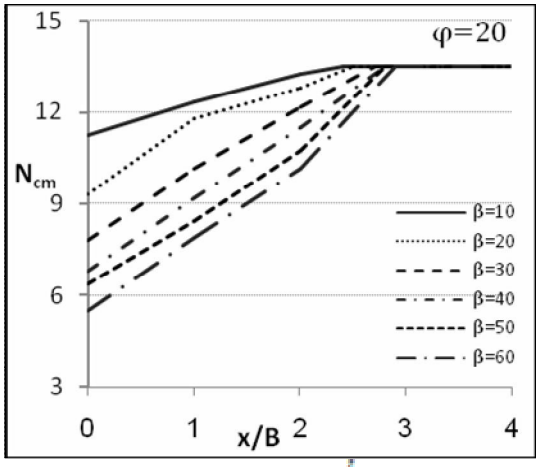

Fig. 24: N_{cm} for ($\frac{L}{B} = 10$)

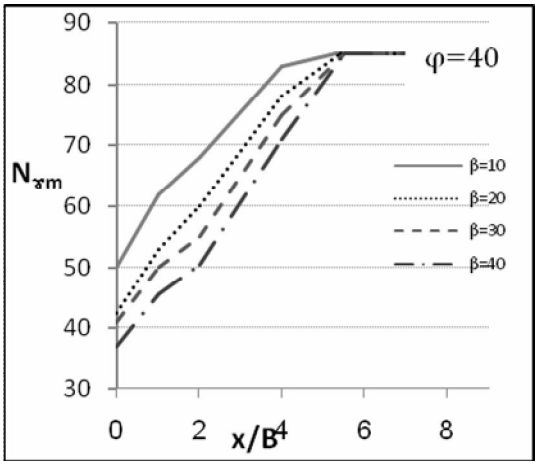

Fig. 25: $N_{\gamma m}$ for square footing

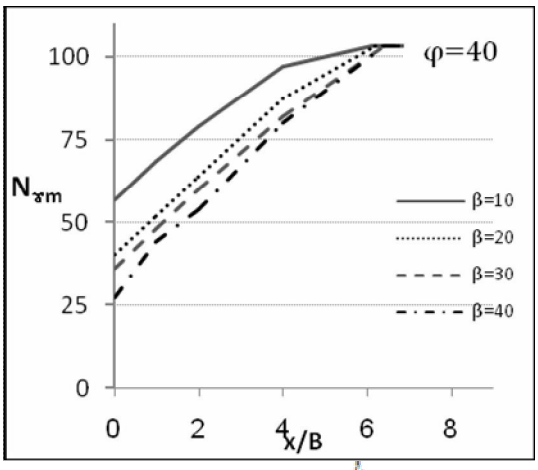

Fig. 28: $N_{\gamma m}$ for ($\frac{L}{B} = 2$)

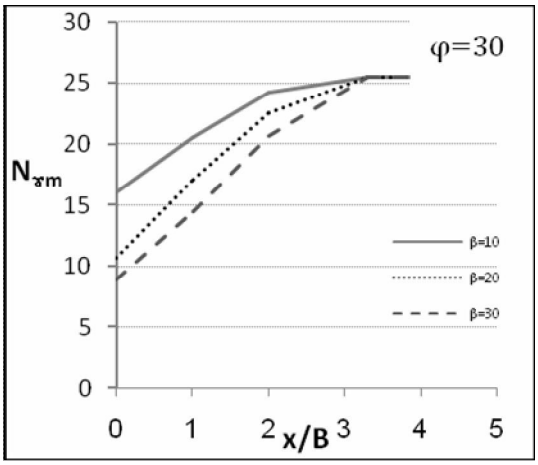

Fig. 26: $N_{\gamma m}$ for square footing

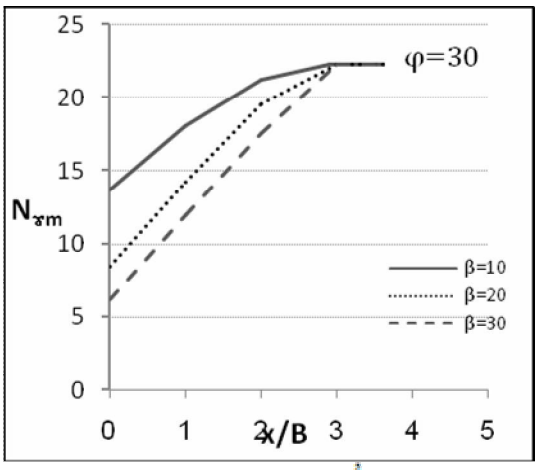

Fig. 29: $N_{\gamma m}$ for ($\frac{L}{B} = 2$)

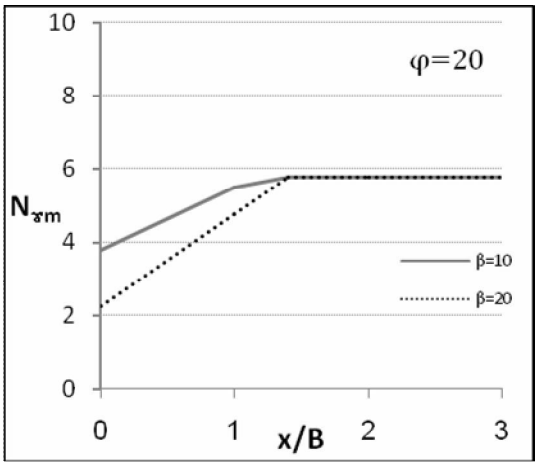

Fig. 27: $N_{\gamma m}$ for square footing

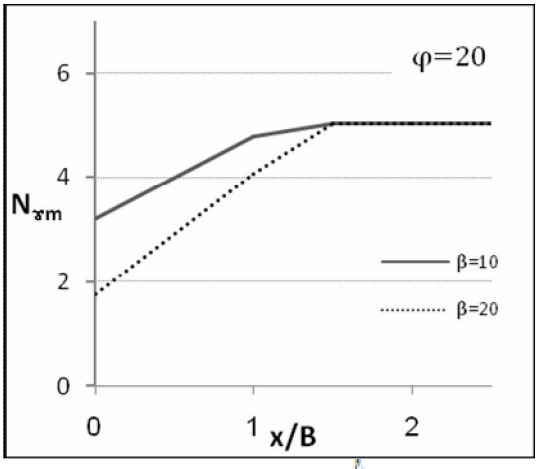

Fig. 30: $N_{\gamma m}$ for ($\frac{L}{B} = 2$)

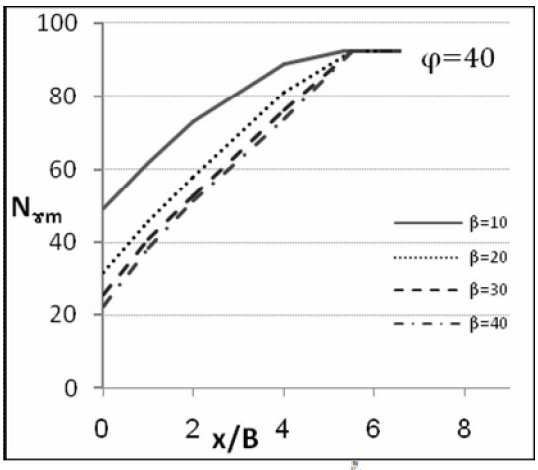

Fig. 31: $N_{\gamma m}$ for ($\frac{L}{B} = 4$)

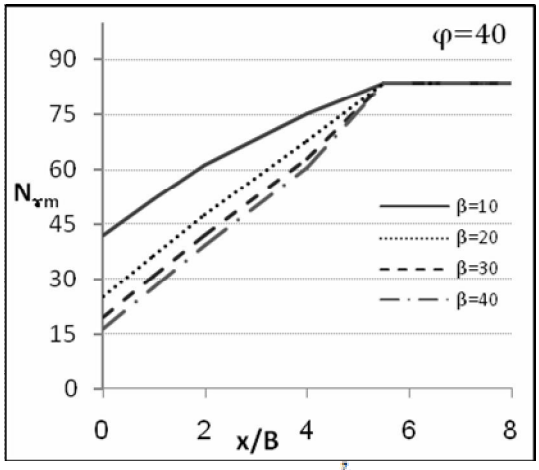

Fig. 34: $N_{\gamma m}$ for ($\frac{L}{B} = 10$)

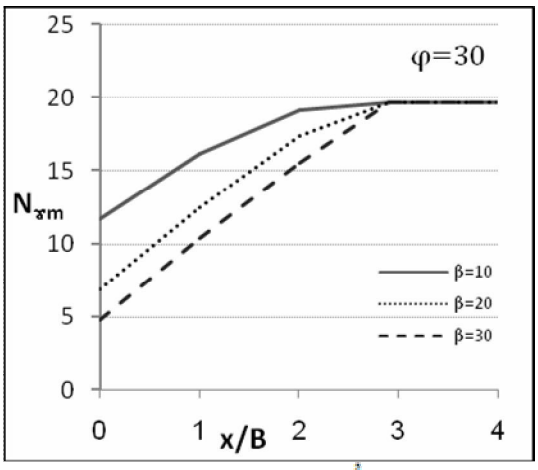

Fig. 32: $N_{\gamma m}$ for ($\frac{L}{B} = 4$)

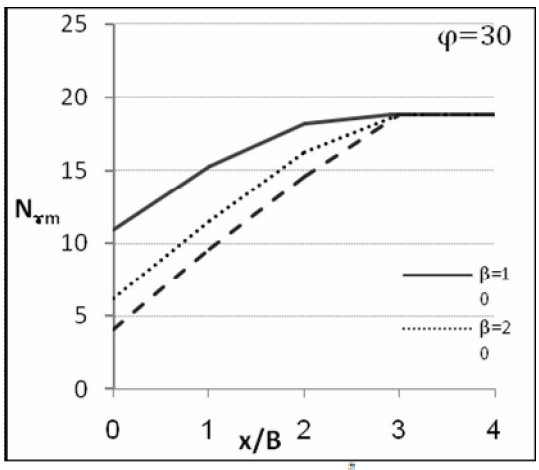

Fig. 35: $N_{\gamma m}$ for ($\frac{L}{B} = 10$)

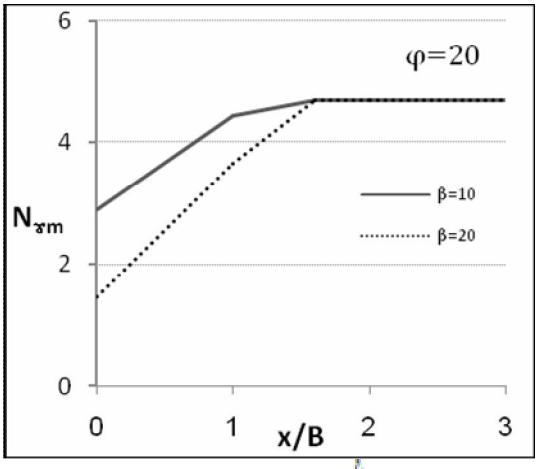

Fig. 33: $N_{\gamma m}$ for ($\frac{L}{B} = 4$)

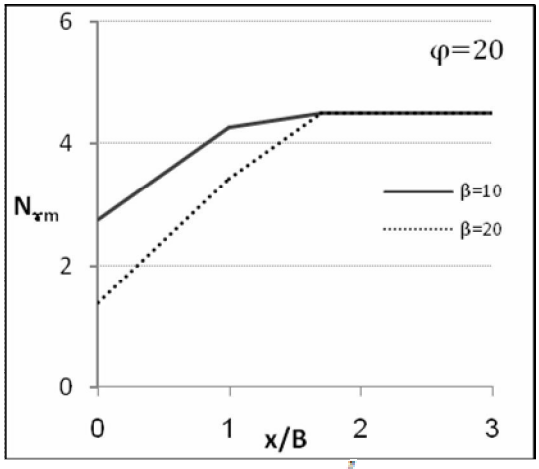

Fig. 36: $N_{\gamma m}$ for ($\frac{L}{B} = 10$)

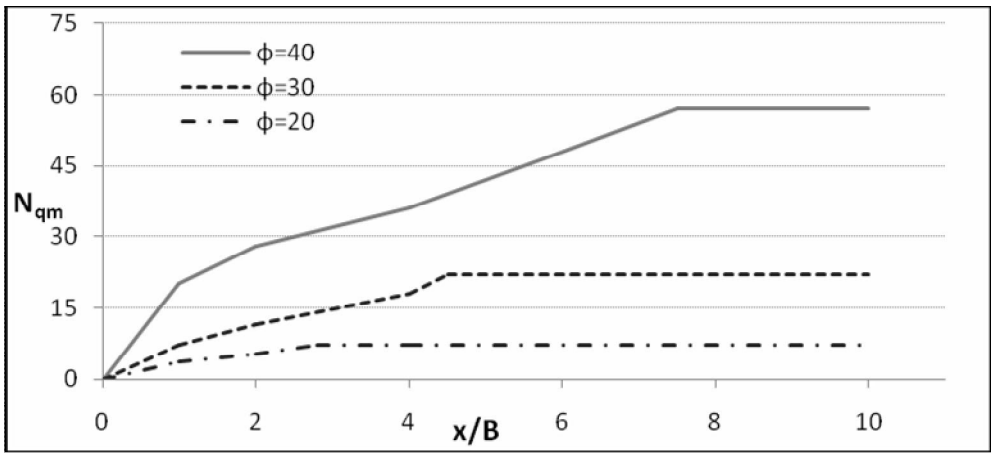

Fig. 37: N_{qm} for square footing

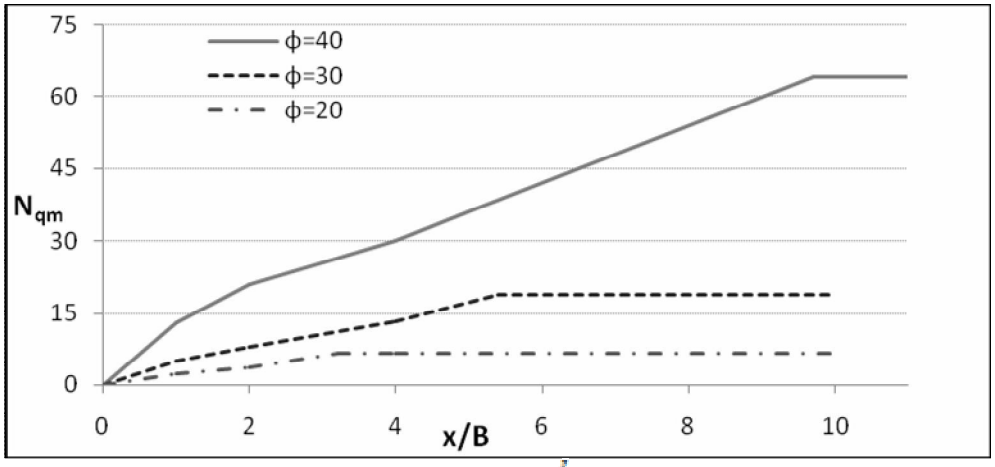

Fig. 38: N_{qm} for ($\frac{L}{B} = 2$)

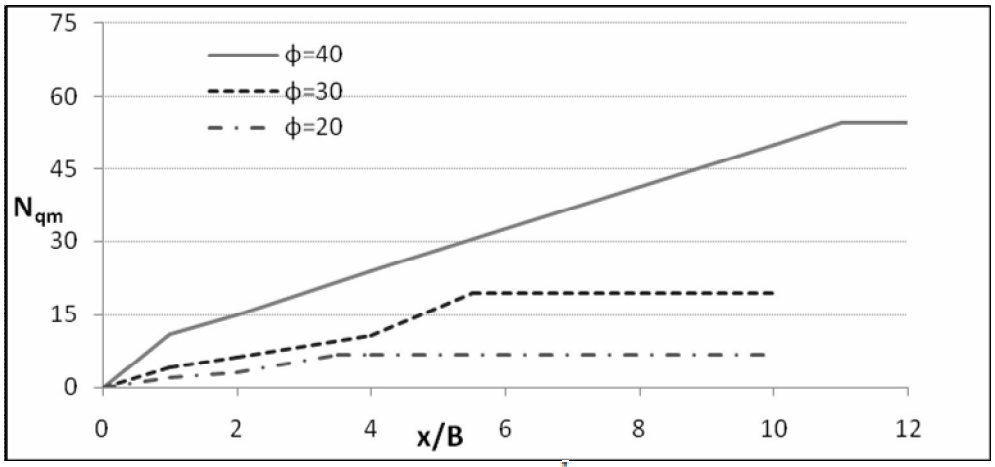

Fig. 39: N_{qm} for ($\frac{L}{B} = 4$)

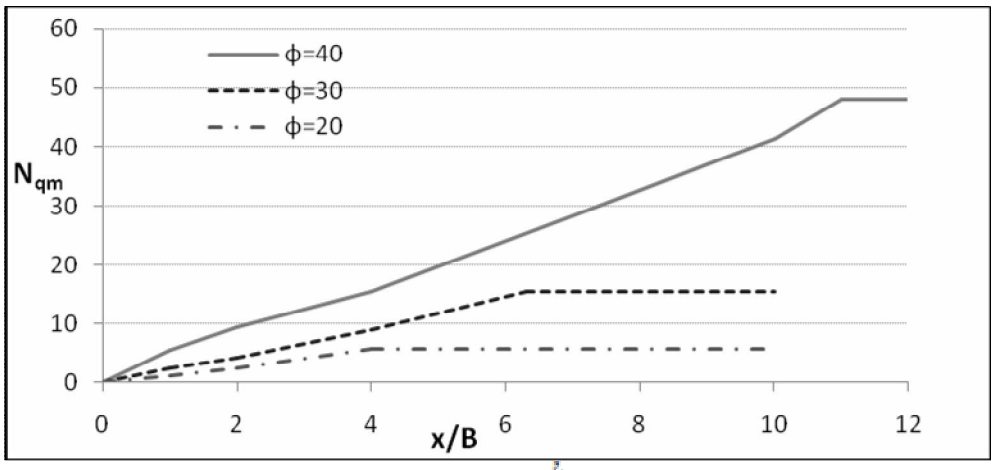

Fig. 40: N_{qm} for ($\frac{L}{B} = 10$)

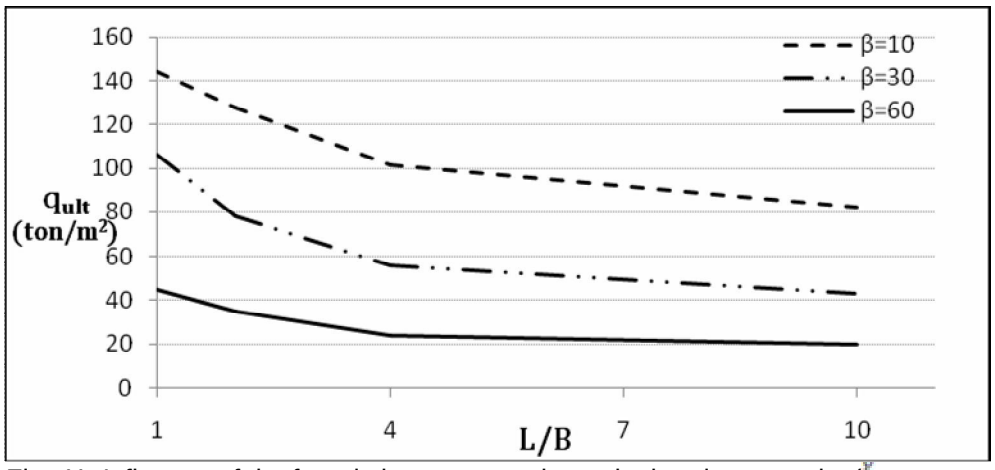

Fig. 41: Influence of the foundation aspect ratio on the bearing capacity ($\frac{x}{B} = 0, \varphi = 40°$)

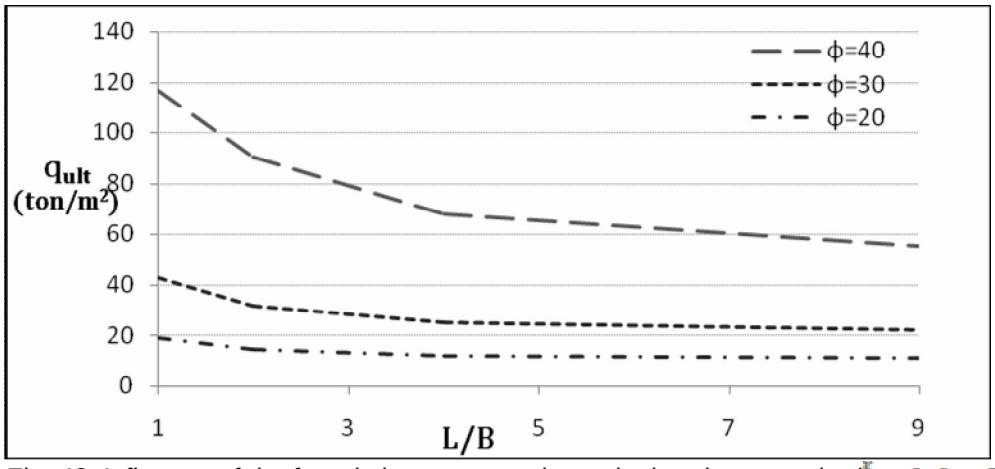

Fig. 42: Influence of the foundation aspect ratio on the bearing capacity ($\frac{x}{B} = 0, \beta = 20°$)

7. REFERENCES

[1] G. G. Meyerhof, “Some Recent Research on the Bearing Capacity of Foundations.” *Canadian Geotech. J.*, 1(1):16-26, 1963.

[2] K. Terzaghi and R. B. Peck, “*Soils Mechanics in Engineering Practice*,” J.Wiley, New York. (1967)

[3] J.B. Hansen, “A Revised and Extended Formula for Bearing Capacity.” *Danish Geotech. Inst. Bulletin,* No. 28, Denmark. 1970.

[4] E.E. De Beer, “Experimental determination of shape factors and the bearing capacity factors of sands,” *Géotechnique,* 20(4) :387-411, 1970.

[5] A.S. Vesic, “Analysis of Ultimate Loads of Shallow Foundations.” *J. of Soil Mech. and Fndn Div.* ASCE, 99(SM1): 45-73, 1973.

[6] R.T. Shield and D.C., Drucker, “The application of limit analysis to punch-indentation problems.” *J. of Appl. Mech.,* ASCE: 453-460, 1953.

[7] A. Nakase, “Bearing capacity of rectangular footings on clays of strength increasing linearly with depth.” *Soils and Foundations*, 21(4): 101-108, 1981.

[8] K. Narita and H.Yamaguchi, “Three-dimensional bearing capacity analysis of foundations by use of a method of slices.” *Soils and Foundations*, 32(4): 143-155, 1992.

[9] K. Ugai, “Bearing capacity of square and rectangular footings on nonhomogeneous clays.” *J. of JSSMFE*, 25(4): 179-185, 1985.

[10] R.L. Michalowski, “Upper-bound load estimates on square and rectangular footings.” *Géotechnique,* 51(9): 787-798, 2001.

[11] R.L. Michalowski, and E.M. Dawson, “Three-dimensional analysis of limit loads on Mohr-Coulomb soil.” *Fndn of Civ. and Inv. Eng., No.* 1: 137-147, 2002.

[12] M. Zhu and R.L. Michalowski, “Shape Factors for Limit Loads on Square and Rectangular footings.” *J. of Geotech. and Geoenv. Eng. ASCE,* 131, No.(2): 223-231, 2005.

[13] R. Salgado, A.V Lyamin, S.W. Sloan, and H.S. Yu, “Two- and three-dimensional bearing capacity of foundations in clay.” *Géotechniqu,* 54(5): 297-306, 2004.

[14] F. Askari and O. Farzaneh, “Upper-bound solution for seismic bearing capacity of shallow foundations near slopes”. Géotechnique, 53(8): 697-70, 2003.

[15] S. K. Sarma and Y. C. Chen, “ Bearing capacity of strip footings near sloping ground during earthquakes”. Proc. 11th world conf. on earthquake engineering, 1989.

[16] P.A. Cundall and O.D.L. Strack, “A discrete numerical model for granular assemblies.” *Géotechnique,* 29(1): 47-56, 1979.

[17] C.S. Chang, “Discrete element method for bearing capacity analysis.” *Comput. and Geotech.,* 12: 273-288, 1991.

[18] C.S. Chang, “Discrete element method for slope stability analysis.” *J. of Geotech. Engng.*, 118(12): 1889-1905, 1992.

[19] C.S. Chang, “Discrete element analysis for active and passive pressure distribution on retaining wall.” *Compu. and Geotech.*, 16: 291-310, 1994.

[20] A.R. Majidi, “Development of the Implicit Three Dimensional Discrete Element Method and Using in Three Dimensional Bearing Capacity Analysis of Shallow Foundations” PHD thesis, University of Tehran, May 2007.

[21] A.R. Majidi and A.A. Mirghasemi, “Iranian Journal of Science and Technology Transaction B-Engineering,32 : 107-124, 2008.

[22] “Aashto LRFD bridge design specifications”, American association of state highway and transportation officials.

[23] A.H. Bozorg Haddad, “3-D study behavior of foundations placed on the slopes by model tests” Master of Science thesis, University of Tehran.